International Journal of Electrical, Electronic and Communication Sciences
ISSN: 2517-9438
Vol:1, No:6, 2007

Perturbations of the EM-field Meters Reading Caused by Flat Roof Security Wall

Alfonso Bahillo, Juan Blas, Santiago Mazuelas, Patricia Fernanadez, Ruben Mateo Lorenzo, and Evaristo Jose Abril

***Abstract*—**The wide increase and diffusion on telecommunication technologies have caused a huge spread of electromagnetic sources in most European Countries. Since the public is continuously being exposed to electromagnetic radiation the possible health effects have become the focus of population concerns. As a result, electromagnetic field monitoring stations which control field strength in commercial frequency bands are being placed on the flat roof of many buildings. However there is no guidance on where to place them. This paper presents an analysis of frequency, polarization and angles of incidence of a plane wave which impinges on a flat roof security wall and its dependence on electromagnetic field strength meters placement.

***Keywords*—**EM field exposition, EM field strength meter, FDTD method, flat roof security wall, plane wave propagation.

I. Introduction

AS a consequence of the increasing electromagnetic (EM) field exposition on human, due to the great development on mobile communications, characterized by an increasing number of users and traffic, the evaluation of EM field in urban environment is assuming an increasing interest. Therefore, competent organizations have assumed the need to protect public health against the possible harmful effects of the exposure to EM fields. In addition, different international organizations, ICNIRP or OMS, based on currently available scientific data and guidelines, have established the basic restrictions and reference levels which should not be exceeded in any inhabited place. As a result, permanent broadband EM field monitoring stations which make frequency selective measurements on different bands from AM (around 1MHz) to Wi-Fi (around 2.4GHz) are being placed on the flat roof of many buildings in order to control the EM field strength and be able to guarantee that human level exposure is in compliance with established rules.

However, there is no guidance on where to place them. Hence, understanding and predicting how flat roof obstacles affect plane wave propagation is a fundamental aspect in the planning of EM field strength meters placement. Similarly, personal exposure meters for assessing exposure to RF (Radio Frequency) electric fields are subject to errors associated with perturbations of the fields by the presence of the human body [1].

Alfonso Bahillo, Juan Blas and Santiago Mazuelas are with CEDETEL (Center for the Development of Telecommunications), Parque Tecnologico de Boecillo, Valladolid (SPAIN), email: abahillo@cedetel.es, jblas@cedetel.es, smazuelas@cedetel.es

Patricia Fernandez, Ruben Mateo Lorenzo and Evaristo Jose Abril are with the Department of Signal Theory and Communications and Telematic Engineering, University of Valladolid, Valladolid (SPAIN), email: patfer@tel.uva.es, rublor@tel.uva.es and ejad@tel.uva.es

This research is partially supported by the Regional Ministry of Education from Castilla y Leon (Spain) under grant VA009B06.

In flat roof environment wave propagation is dominated by man-made walls, air conditioner equipment and other obstacles. As we will see in this paper, when the plane wave reaches an isotropic receiving probe after penetrating through, scattering of or reflecting from flat roof obstacles, the EM field strength can fluctuate from -10dB to 2dB because of attenuation, constructive and destructive interferences. These differences from field strength in free space become stronger when the obstacles size is comparable with wavelength size. Consequently, the place where the monitoring station is located on the flat roof is very important in order to avoid that the appropriate organizations make decisions based on wrong measurements or measurements influenced by flat roof obstacles. In this paper a security wall around the flat roof is analyzed. A confidence threshold is established in order to ensure that the measurement error received by isotropic probe and caused by flat roof security wall on plane wave propagation will be under 5%. This error is defined to be the difference between the incident wave strength being measured and the RF meter reading.

By using computer simulations it is possible to predict the location of these problem areas, thereby it gives us the possibility to optimize the placement of measure equipment. Numerical simulations have been performed with 3-D finite-difference time-domain (FDTD) method to analyze the plane wave-wall interaction problem. Time-domain analysis appears to be attractive because the time-dependent analysis approaches can provide the complete time evolution of the process as a plane wave interacts with a concrete wall [2]-[3].

The goal of this paper is to understand the local interaction behavior of a time-domain plane wave at different wave polarizations, frequencies and angles of arrival, with a security wall around the flat roof which is composed of brick and a waterproofing material covered with a thin metallic coat on its inner side. Our aim is to establish a confidence threshold in measurement equipment placement in order to ensure that measurements are not influenced by that wall and thus provide the appropriate organizations guidance on monitoring station placement.

II. Numerical Method of Analysis

In this paper, numerical simulations are performed with 3-D FDTD algorithm because it is simple to understand and can be used to analyze complex structures. As the FDTD method is well known and is described in [4], only a brief outline will be presented here. The first step in designing a flat roof wall with an FDTD code is to grid up the structure making a 3-D grid

with integer numbers in their nodes where each integer number represents a kind of material and each material is identified with its electrical properties, ε (realtive permittivity) and σ (electrical conductivity) at each frequency (See Table *I* and Table *II*).

The sampling nodes must be taken to ensure that an adequate representation is made. A good rule of thumb is 10 points per wavelength [5]. At the highest frequency, 1800MHz, the spatial increment must be minor than λ/10=16mm. But, in order to depict the model without omitting any material of the structure, the cell width must be equal or inferior to 2mm. Because of EM field is sharing out at each half spatial increment, we have to consider that the unit cell is divided into two parts, therefore, cell width will be set to Δx=4mm. Once spatial increment size is chosen, in order to avoid numerical instabilities, time step is fixed to Δt=$\Delta x/2c_0$ which satisfy the well-known Courant condition of scheme stability [6]. The total number of time steps has been chosen based on the total length the plane wave has to travel in order to cover the whole computational domain. For example, as we will see in section III, we have chosen 6500 time steps when α=0 and the plane wave has to travel a distance of 330cm. In the simulations we probed that the number of time steps chosen is enough simulation time to have died out the plane wave from the computational volume.

Let us consider a Gaussian pulse in the time domain like a excitation source (1), which if it is narrow enough, is a good approximation to an impulse:

$$V(t) = e^{-\frac{1}{2}(\frac{(T_0-t)}{\sigma})^2} \quad (1)$$

where the parameters are T_0=20ps and σ=6.

System theory tell us that we can get the response to every frequency if we use an impulse like initial source. But we have to repeat the simulation for each frequency because of frequency dependence of materials dielectric constant and electrical conductivity which make up the flat roof wall. Therefore, it will be necessary to load on grid nodes the dielectric constant and electrical conductivity of each material at each simulation frequency. After waiting for having died out the pulse, we take the Fourier transform of the total electric field at the frequency of interest with regard to the Fourier transform of the incident source. As a result, we know the relation between the total electric field strength and the incident source strength over each grid node and at each work frequency.

In order to avoid that the EM field was reflected in the limits of the computational domain and it came back to simulation volume, it is necessary to define an absorbing boundary condition which keeps outward the EM field after reaching the edge of the allowable volume. One of the most flexible and efficient absorbing boundary conditions is the perfectly matched layer (PML) developed by Berenger [7]. In this paper, we have made use of 15 PML layers, which are long enough to absorb the power that reaches the edge of the problem space.

III. Model Description

Nowadays it is common to find a flat roof at the top of many big buildings with a security wall around it. In this paper, the analyzed structure is a brick-wall of a flat roof hit by a plane wave, therefore we are assuming far field. Computational volume is $X_v \times [Y_v + Y_{r_0}] \times Z_v$ which is closed by PML absorbing boundary and where X_v=40cm, Y_v=50cm, Y_{r_0}=280cm, and Z_v=140cm, when α=0

In Fig.1 we show the model we are going to use in simulations. It represents a flat roof lateral, which consists of a exterior brick-wall where we can observe a concrete ledge as its upper bound. In the inner side of the wall it is placed a waterproofing material which is covered with a thin metallic coat. Flat roof floor is constituted of various layers, the first one is made of boulders followed by a cotton blanket, a rigid wood layer and a cork one to protect the waterproofing layer. The last one is set to isolate from water the roof of the building.

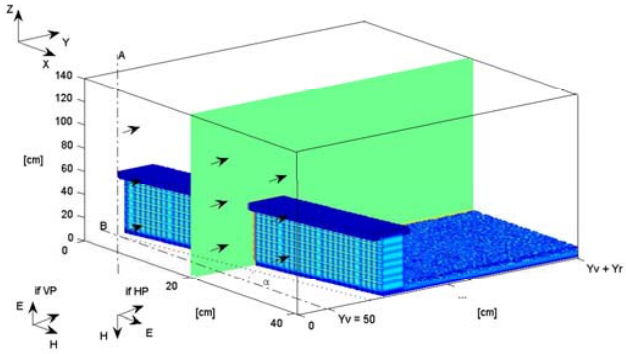

Fig. 1: Three-dimensional (3-D) flat roof wall computational volume [cm×cm×cm]. Y=0, illuminating plane. X=20, outcome visualization plane.

A fundamental aspect in model description is computational volume size choice, in particular, the amount of vacuum that we have to consider in front of and above the wall, as far as computational resources limitation is concerned. As we can see in Fig.1, the structure does not change along the longitudinal section of the wall. For this reason and in order to minimize computing time and the computational storage, we have decided to reduce X axis length until 40cm, which is long enough compared with wavelength size at the most relevant frequency, 1800MHz. Because of plane wave scattering on wall ledge, the Y and Z axes size has been chosen based on the resulting shadow distance from the wall at the highest simulation frequency. In simulations terms, Y=0 is the illumination plane while X=20 is the outcome visualization plane. Therefore, taking advantage of the fact that the structure does not change along the longitudinal section of the wall, when $\alpha \neq 0$, in order to be able to compare simulation results with different values of α taking the same visualization plane, X=20, the computational volume is lengthened in the Y direction up to Y_v+Y_r where Y_r=$(X_v/2)tan(\alpha)$+$Y_{r_0}/cos(\alpha)$, as is shown in Fig.1. After that, the Y axis in the outcome

visualization plane is scaled-down according to α value.

The electrical conductivity and relative permittivity values chosen from different materials used at each interest frequency have been collected in Table *I* and Table *II*.

TABLE I
RELATIVE PERMITTIVITY (ε)

	100 MHz	900 MHz	1800 MHz
Material	ε	ε	ε
Vacuum	1	1	1
Concrete	4.75	4.52	4.1
Aluminium	10	10	10
Waterproofing	3	2.9	2.7
Boulders	4.7	4.49	3.9
Cork	1.55	1.52	1.47
Brick	8	7	5
Cotton	1.35	1.35	1.35
Wood	6.8	5.3	2.3

TABLE II
ELECTRICAL CONDUCTIVITY (σ) [S/M]

	100 MHz	900 MHz	1800 MHz
Material	σ	σ	σ
Vacuum	0	0	0
Concrete	0.025	0.065	0.13
Aluminium	3.54×10^{7}	3.54×10^{7}	3.54×10^{7}
Waterproofing	1×10^{-14}	1×10^{-13}	1×10^{-12}
Boulders	0.026	0.07	0.13
Cork	1.2×10^{-10}	1.2×10^{-10}	1.2×10^{-10}
Brick	0.02	0.022	0.3
Cotton	1×10^{-10}	1×10^{-10}	1×10^{-10}
Wood	0.005	0.006	0.007

Characteristics of the computational volume have been examined for varying plane wave polarization, the frequency (100, 900 and 1800MHz), different angles of incidence and modifying the possible presence of the thin metallic coat. In all simulation tests, we have used a monochromatic plane wave with vertical (VP) or horizontal (HP) polarization. The illuminating plane of the problem space has been Y=0 where the wavefront travels toward positive values of Y at each time step. In order to have more control over electric and magnetic field behavior in wall vicinities, we have varied the angle of incidence of the plane wave. Instead of modifying the wavefront phase which illuminates the flat roof wall, we have rotated the flat roof structure by using the A and B axes shown in Fig.1. In this way we have been able to simulate changes both in azimuth and inclination arrival angles respectively.

If we revolve the structure around the B axis clockwise, we are capturing the influence of a plane wave which comes from an EM source situated below the horizontal plane of the flat roof. This will be a future work where EM field strength at the top of the building coming from pico cells would be observed. Thus, we could see if it is relevant or not and what dynamic range a monitoring station would need in order to capture the influence of this kind of sources. If we revolve the structure around the B axis counter-clockwise, we are capturing the influence of a plane wave which comes from an EM source situated above the horizontal plane of the flat roof. But in this case, we have checked that the resulting shadow size is always minor than the resulting one when the source is situated in the horizontal plane. Therefore, in section V we will compare the diffraction pattern generated when a plane wave hits the wall of the flat roof for different incident azimuth angles with no rotation around B axis.

IV. RESULTS

After illuminating the flat roof model with a plane wave at 1800MHz we can see in an easy way the disturbance of the plane wave propagation which is caused by the wall presence. In Fig.2 we can notice this effect for two different polarizations, vertical and horizontal plane wave polarization and in Fig.3 we can notice the effect of different azimuth angles of incidence.

In both Fig.2 and Fig.3 we can see that in front of the wall it takes place constructive and destructive interferences, having as a result a stationary waveform due to reflections and scattering on the wall. As we can see in Fig.3 these interferences diminish as the azimuth angle of incidence increases.

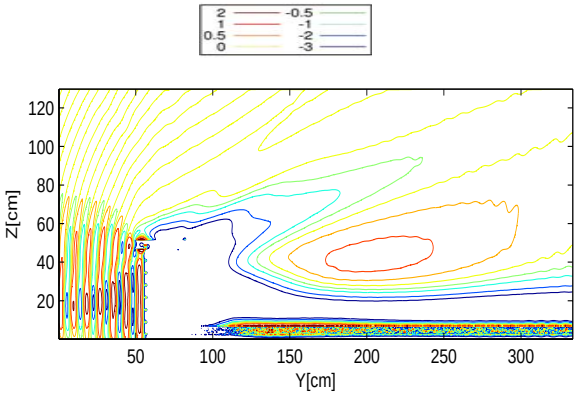

(a) Vertical Polarization

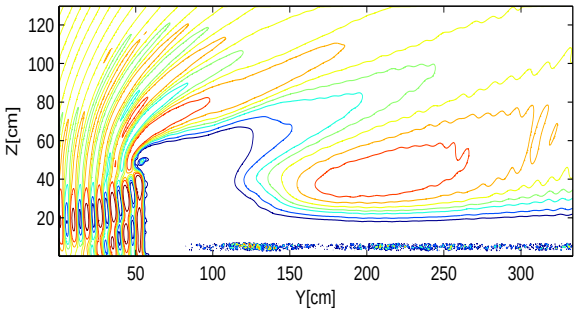

(b) Horizontal Polarization

Fig. 2: Total EM field strength [dB] with regard to incident wave at 1800MHz and α=0. Cross section of the computational domain by plane X=20.

As we can see in Fig.2, when the polarization of the incident wave is orthogonal to the wall edge, Fig.2(a), the shadow size behind the wall is lower than when the incident wave polarization is parallel to it, Fig.2(b). When the polarization of the incident wave is parallel to the wall edge, the plane

wave has more difficulties to reach the places situated behind it because the scattering process is more severe. For this reason the resulting shadow behind the wall edge is bigger when the plane wave has horizontal polarization.

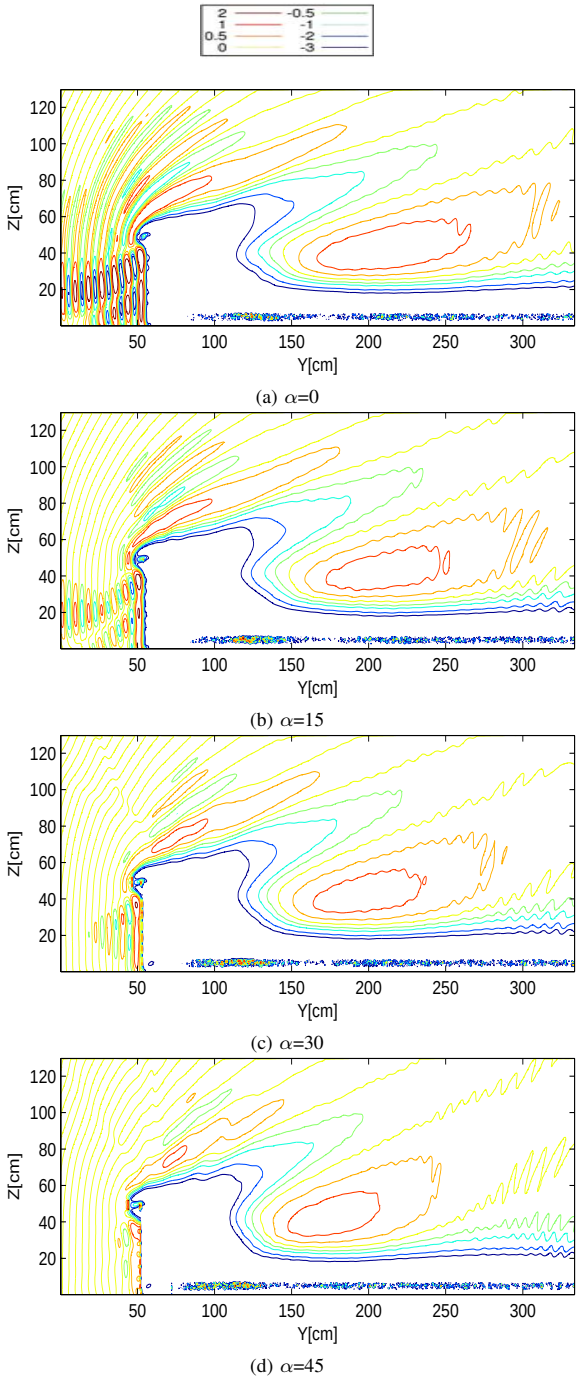

Fig. 3: Total EM field strength [dB] with regard to incident wave at 1800MHz and Horizontal Polarization. Cross section of the computational domain by plane X=20.

On the other hand, if we vary the azimuth angle of incidence, when we revolve the structure around the A axis clockwise or counter-clockwise, we can see that the higher the azimuth angle, the smaller the resulting shadow size behind the wall. That is because if the electric field vector of the plane wave is separated into two components, the orthogonal and the parallel to the wall, the component of the plane wave which impinges parallel to the wall is minor as the angle of incidence increases compared with the component which impinges parallel to it when α=0.

In the results shown in Fig.2 and Fig.3, the fluctuations of the level lines at the end of the computational volume in Y direction are due to small reflections which take place at the end of the allowable space because the absorbing boundary conditions are not perfect. These fluctuations are higher as far as α increases because of scaling-down.

V. Discussion

We have established a threshold over which we can guarantee that flat roof wall influence on plane wave propagation is under 5% with regard to EM field strength in free space. This threshold is related to the scattering of the plane wave over the wall.

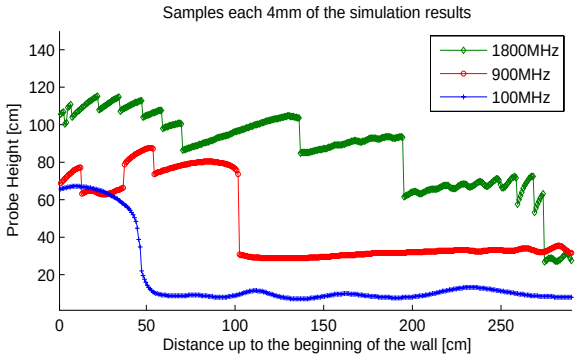

Fig. 4: Threshold over which the influence of the wall on plane wave propagation at 100, 900 and 1800MHz with Horizontal Polarization is under 5% with regard to EM field strength in free space.

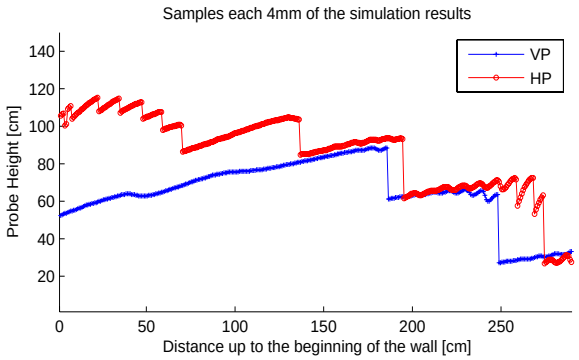

Fig. 5: Threshold over which the influence of the wall on plane wave propagation at 1800MHz is under 5% with regard to EM field strength in free space. Vertical and Horizontal Polarization.

As it was expected, the higher the frequency, the wall size becomes an obstacle comparable to wavelength size. That is why the influence of the wall on plane wave propagation is more relevant at 1800MHz. As far as frequency increases, most EM field behind the wall comes from its going over that wall, not from going through it. As we can see in Fig.4 the scattering over the wall edge generates a shadow behind it, whose size increases with simulation frequency.

As we showed in section IV, the resulting shadow behind the wall edge when the plane wave has vertical polarization is less than when the plane wave has horizontal polarization because the direction of polarization is orthogonal to the wall edge with vertical polarization. This result is shown more clearly in Fig.5 where we can see that the threshold above which the influence of the wall on plane wave propagation is under 5%, is minor when the plane wave has vertical polarization.

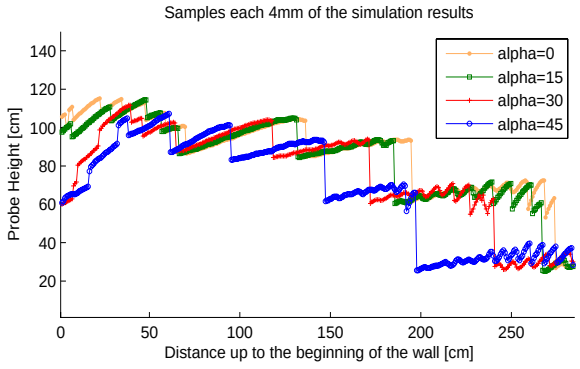

(a) Samples each 4mm of the simulation result in Y direction.

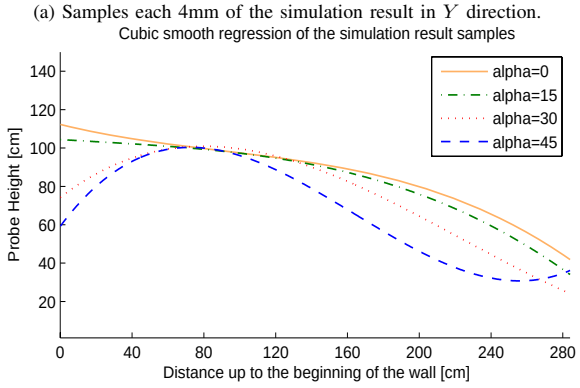

(b) Cubic smooth regression of the simulation result samples.

Fig. 6: Threshold over which the influence of the wall on plane wave propagation at 1800MHz with Horizontal Polarization is under 5% with regard to EM field strength in free space. Different azimuth angles of incidence.

On the other hand, in Fig.6, at 1800MHz and when the plane wave has horizontal polarization, we compare the resulting threshold when the azimuth angle of incidence is increased. As we said in section IV, we can see that the larger the azimuth angle of incidence, the lower the resulting threshold (see Fig.6(a)). This can be seen in an easy way in Fig.6(b) where we use a cubic smooth regression of the samples showed in Fig.6(a) that is the third degree polynomial which best fits the samples available minimizing its curvature.

Another important result is that at 1800MHz, the observed differences when plane wave is coming from Y=0 plane, between putting or not putting the metallic coat on plane wave propagation are negligible. This result strengthen the idea by which most EM field behind the wall comes from its going over that wall, not from going through it.

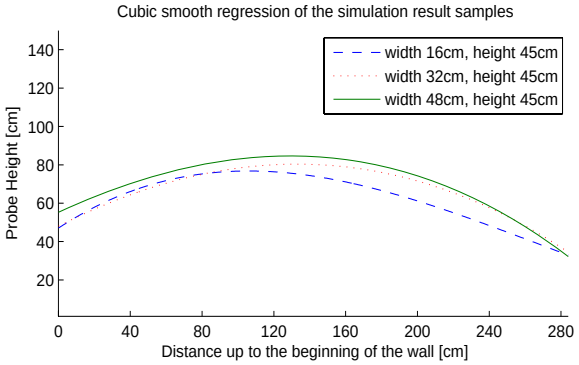

(a) Changing wall width.

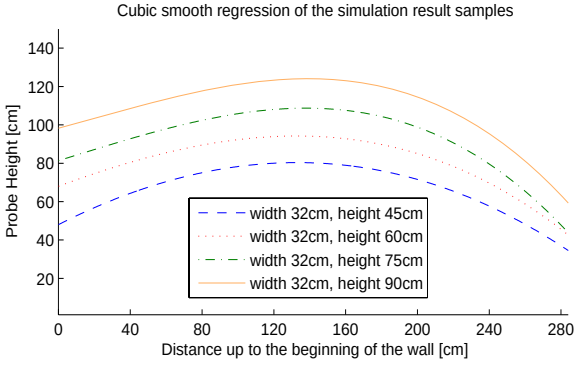

(b) Changing wall height

Fig. 7: Threshold over which the influence of the wall on plane wave propagation at 1800MHz is under 5% with regard to EM field strength in free space. Plane wave with Vertical Polarization. Different wall size.

Equally important and with the aim to generalize results, we have changed the height and width of the wall. Simulation results are shown in Fig.7, where we use a cubic smooth regression which best fits the samples available. In it, we can see that at 1800MHz and with vertical polarization, the shadow caused by plan wave scattering over the wall edge remains constant with height and width wall variation. Therefore, we can make simulation results independent from flat roof wall size.

In results showed in this paper, the most restrictive situation in monitoring station probe placement is concerned, takes place when the plane wave has horizontal polarization, the angle of incidence is α=0 and with the highest simulation frequency, 1800MHz. In this situation the monitoring station probe should be placed over the red line in Fig.6(b) which gives us a smooth version on threshold placement.

VI. Conclusion

Based on the FDTD method, the effects of a flat roof security wall with a waterproofing material covered by a thin metallic coat on wave propagation are studied in this paper. Characteristics of the computational volume have been examined for varying plane wave polarization, the frequency, different angles of incidence and modifying the presence of the metallic coat. Simulations results show us that the most restrictive situation in monitoring station probe placement is concerned, takes place with horizontal polarization, no rotations of the structure around A or B axes and with the highest simulation frequency, 1800MHz. Moreover, we can make simulation results independent from flat roof wall size

Detailed simulation results are presented, which are helpful for practical monitoring station positioning and useful for better understanding the behavior of the far field in flat roof wall vicinities. These results shown us that compared with EM filed strength in free space, the EM field in flat roof vicinities can fluctuate from -10dB to 2dB. Therefore, is very important where to place the EM field strength meters in flat roof vicinities. Avoiding ambiguous places we will be able to obtain clearer results as far as EM field strength over flat roof buildings is concerned.

References

[1] J. Blas, F. A. Lago, P. Fernandez, R. M. Lorenzo and E. J. Abril, *Potential exposure assessment errors associeted with body-worn RF dosimeters (to be published)*, Bioelectromagnetics Wiley-Liss, Inc.

[2] R. A. Dalke, C. L. Holloway, P. McKenna, M. Johansson, and A. S. Ali, *Effect os Reinforced Concrete Structures on RF Communications*, IEEE Trans. Electromagn Compat, Vol.42,pp.486-496. 2000.

[3] G. Antonini, A. Orlandi, S. Delia, *Shielding Effects of Reinforced Concrete Structure to Electromagnetic Fields due to GSM and UMTS Systems*, IEEE Trnas. Magnetics, Vol.39,pp.1582-1585. May 2003.

[4] K. S. Yee, *Numerical solution of initial boundary value problems involving Maxweell's equations in isotropic media*, IEEE Trans. Antennas and Propagat., vol. 17, 1966, pp.585-589.

[5] A. Taflove, *Computation Electrodynamics: The Finite-Difference Time-Domain Method*, Boston, MA: Artech House, 1995.

[6] K. S. Kunz and R. J. Luebbers, *The Finite Difference Time Domain Method for Electromagnetics*, Boca Raton, FL; CRC Press, 1993.

[7] J. P. Berenger, *A perfectly matched layer for the absortion of electromagnetic waves*, J. Compput. Phys.,vol. 114, 1994, pp. 185-200.

[8] D. M. Sullivan, *Electromagnetic simulation using the FDTD method*, New York, NY: IEEE Press, July 2000.